

# Photoproduction of $\eta$ and $\eta'$ mesons with EtaMAID

Lothar Tiator<sup>1,\*</sup>, Viktor Kashevarov<sup>1</sup>, and Michael Ostrick<sup>1</sup>

<sup>1</sup>*Institut für Kernphysik, Johannes Gutenberg-Universität Mainz, Mainz, Germany*

**Abstract.** The unitary isobar model EtaMAID has been updated with an extended list of nucleon resonances, fitted to recent and new data for differential cross sections and polarization observables. The nonresonant background is described by Regge trajectories of  $\omega, \rho$  and  $a_1, b_1$  mesons and in addition Regge cuts, where vector and axial vector mesons are exchanged together with Pomeron and  $f_2$  mesons.

## 1 Introduction

The isobar model EtaMAID is an online program [1] of the MAID collaboration in Mainz for calculations of observables, amplitudes and multipoles for  $\eta$  and  $\eta'$  photo- and electroproduction on the nucleon. It was introduced in 2001 [2] and updated in 2003 [3]. Here we will present a new update EtaMAID2016, in progress, taking into account very recent high-precision data of differential cross sections for  $p(\gamma, \eta)p$  and  $p(\gamma, \eta')p$  from MAMI [4] and polarization observables with beam and target polarization from MAMI [5], ELSA [6], JLab [7] and GRAAL [8]. The high-energy region  $W > 2$  GeV is set up with Regge trajectories and Regge cuts and can well describe all high-energy data including polarization observables for  $\gamma, \pi^0, \gamma, \eta$  and  $\gamma, \eta'$ . In the resonance region below  $W \approx 2$  GeV we investigated more than 20  $N^*$  resonances and found significant contributions for 18 of them. A very good description has been obtained for all existing photoproduction data.

## 2 EtaMAID2016

In the spirit of the unitary isobar model MAID for pion photo- and electroproduction [1], the EtaMAID model is set up in the following way

$$t_{\gamma\eta}(W) = t_{\gamma\eta}^{bg}(W) + t_{\gamma\eta}^R(W), \quad (1)$$

with a background and a resonance  $t$ -matrix term. The background is described in a field-theoretical approach with Feynman diagrams for Born  $s$ - and  $u$ -channels and vector-meson  $t$ -channel exchanges. The resonance part is described with resonance excitations for individual partial waves, where in our current work partial waves up to  $G$  waves are considered. Due to isospin zero of  $\eta$  and  $\eta'$  mesons,  $\Delta$  resonances can not be excited.

Of course, this ansatz is not unique. However, it is a very important prerequisite to clearly separate resonance and background amplitudes within a Breit-Wigner concept also for higher and overlapping resonances.

---

\*e-mail: tiator@kph.uni-mainz.de

## 2.1 Regge approach for background

In the asymptotic region,  $E > 3$  GeV, the Regge regime, the  $t$ -channel vector meson exchange contributions can be replaced by Regge trajectories. This is easily been done by replacing the meson propagator in the  $t$ -channel Feynman diagrams by the Regge trajectories, Fig. 1, e.g. for vector-meson exchanges of  $\rho$  and  $\omega$  [3]

$$\frac{1}{t - M_\rho^2} \Rightarrow D_V = \left( \frac{s}{s_0} \right)^{\alpha_V(t)-1} \frac{\pi \alpha'_V (e^{-i\pi\alpha_V(t)} - 1)}{2 \sin[\pi\alpha_V(t)] \Gamma[\alpha_V(t)]}, \quad (2)$$

where we have already applied the signatures  $\mathcal{S} = -1$  of the Regge trajectories for  $\rho$  and  $\omega$ . For  $b_1$  and  $a_1$  axial vector exchange, the signatures of the Regge trajectories are also -1 and the propagators  $D_A$  have the same form.

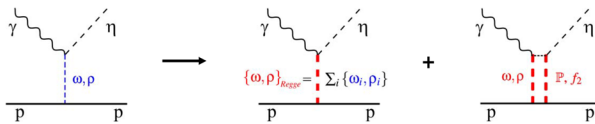


**Figure 1.**  $t$ -channel vector meson exchange diagrams for Regge contributions in pseudoscalar meson photoproduction. The standard Feynman diagram for single poles is replaced by Regge trajectories and Regge cuts with the simultaneous exchange of two Reggeons.

As Donnachie and Kalashnikova [9] suggested, in addition to Regge trajectories, also Regge cuts, Fig. 1, play an important role and can even dominate. These Regge cuts can be considered as a box diagram, where always 2 particles are exchanged,  $\rho\mathcal{P}$ ,  $\rho f_2$  and  $\omega\mathcal{P}$ ,  $\omega f_2$ , where  $\mathcal{P}$  is the Pomeron with quantum numbers of the vacuum and  $f_2$  are tensor mesons with quantum numbers  $0^+(2^{++})$ . All four Regge cuts can contribute to vector and axial vector exchanges and can be written in the following form

$$D_{cut} = \left( \frac{s}{s_0} \right)^{\alpha_c(t)-1} e^{-i\pi\alpha_c(t)/2} e^{d_c t}. \quad (3)$$

In total, the vector meson propagators are replaced by

$$D_V = D_V + c_{VP} D_{VP} + c_{Vf} D_{Vf}, \quad V = \rho, \omega \quad (4)$$

and the axial vector meson propagators are replaced accordingly. The coefficients  $c_\alpha$  for natural and unnatural parity cuts are obtained by a fit to the data. Born terms are not required in the fit.

In Fig. 2 we show the forward cross sections at small  $t$  for high energy  $\eta$  photoproduction. The dip around  $t \approx -0.6$  GeV<sup>2</sup> shows the typical Regge behavior for trajectories with signature -1. This dip region is filled by the Regge-cut contributions and describe the data very well. No Born terms and  $N^*$  resonances are included here.

## 2.2 Breit-Wigner ansatz for resonance excitations

Due to isospin zero of  $\eta$  and  $\eta'$  only  $N^*$  resonances with isospin 1/2 can be excited. Whereas in the original EtaMAID2001 and also in 2003 only 8 resonances were found to contribute (dominant contributions from:  $S_{11}(1535)$ ,  $D_{13}(1520)$ ,  $S_{11}(1650)$ ,  $D_{15}(1675)$ , sub-dominant from

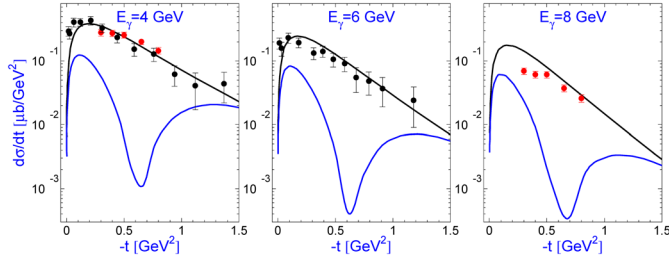


**Figure 2.** Forward (small  $t$ ) differential cross sections for  $\eta$  photoproduction described by Regge contributions. The blue lines show the contribution with  $\rho, \omega$  Regge trajectories alone, giving rise to a pronounced dip, whereas the black lines give the total Regge contribution including the cuts. The data are from [10] (black) and [11] (red).

$F_{15}(1680), D_{13}(1700), P_{11}(1710), P_{13}(1720)$ ), we have now investigated the sensitivity of up to 20  $N^*$  resonances, practically all known resonances of the Particle Data Tables [12].

The relevant multipoles  $\mathcal{M}_{\ell\pm}(E_{\ell\pm}, M_{\ell\pm})$  are assumed to have a Breit-Wigner energy dependence of the following form

$$\mathcal{M}_{\ell\pm}(W) = \bar{\mathcal{M}}_{\ell\pm} f_{\gamma N}(W) \frac{M_R}{M_R^2 - W^2 - iM_R\Gamma_{\text{total}}(W)} f_{\eta N}(W) C_{\eta N}, \quad (5)$$

where  $f_{\gamma N}(W)$  and  $f_{\eta N}(W)$  are Breit-Wigner factors describing the  $\gamma N$  and  $\eta N$  vertex of an  $N^*$  resonance with spin  $J$  and partial width  $\Gamma_{\eta N}(W)$

$$f_{\gamma N}(W) = \left( \frac{k_\gamma}{k_{\gamma,R}} \right)^2 \left( \frac{X^2 + k_{\gamma,R}^2}{X^2 + k_\gamma^2} \right)^2 \quad \text{and} \quad f_{\eta N}(W) = \zeta_{\eta N} \left[ \frac{k_\gamma}{(2J+1)\pi} \frac{M_N}{M_R} \frac{\Gamma_{\eta N}}{q_\eta} \right]^{1/2}, \quad (6)$$

with  $k_\gamma$  and  $q_\eta$  the photon and  $\eta$  meson momenta in the c.m. system, and  $\zeta_{\eta N} = \pm 1$  a relative sign between the  $N^* \rightarrow \eta N$  and  $N^* \rightarrow \pi N$  couplings.  $C_{\eta N}$  is an isospin factor, which is  $-1$  for  $\eta N$  and  $\eta' N$  final states.

The total width is a sum over 7 possible decay channels

$$\Gamma_{\text{total}}(W) = \Gamma_{\pi N}(W) + \Gamma_{\pi\pi N}(W) + \Gamma_{\eta N}(W) + \Gamma_{K\Lambda}(W) + \Gamma_{K\Sigma}(W) + \Gamma_{\omega N}(W) + \Gamma_{\eta' N}(W). \quad (7)$$

The partial decay widths are typically parameterized in the following way, e.g. for  $\eta N$ ,

$$\Gamma_{\eta N}(W) = \beta_{\eta N} \Gamma_R \left( \frac{q_\eta}{q_{\eta,R}} \right)^{2\ell+1} \left( \frac{X^2 + q_{\eta,R}^2}{X^2 + q_\eta^2} \right)^\ell, \quad (8)$$

where  $X$  is a damping parameter. In EtaMAID2003 it was assumed to be constant 500 MeV for all resonances and all partial widths, but in our current work we are using  $X$  as a fit parameter. The c.m. momenta, taken at the resonance position,  $W = M_R$ , are denoted by an additional index  $R$ . In the EtaMAID update we also included further 2-body decay channels, namely  $K\Lambda, K\Sigma, \omega N$ . Branching ratios for  $\eta N$  and  $\eta' N$  are fitted to the data of  $\eta$  and  $\eta'$  photoproduction, for all other channels the pure sensitivity of the branching ratios in the total width is not enough to get reliable fits, therefore, these numbers were taken from PDG [12] and from a coupled-channels partial wave analysis [13].

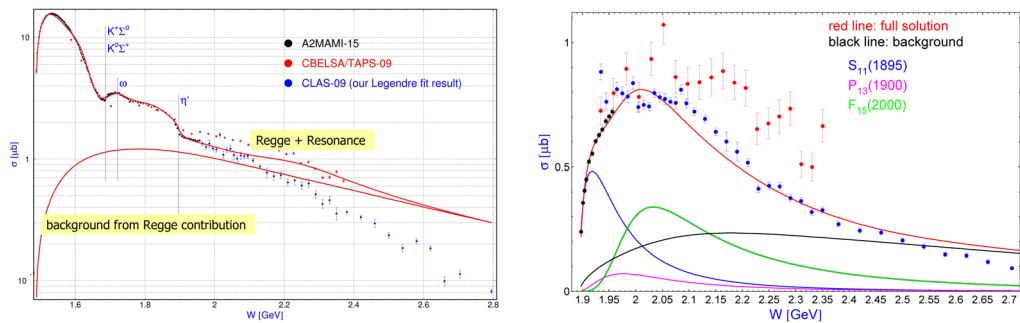


**Figure 3.** Total cross section for  $\eta$  (left) and  $\eta'$  (right) photoproduction on the proton. In both figures the Regge background and the total contributions are shown. For  $\eta'$  photoproduction we also give the dominant contributions from individual resonances,  $N(1895)1/2^-$  (blue),  $N(1900)3/2^+$  (magenta) and  $N(2000)5/2^+$  (green). The data are from Mainz [4], Bonn [6] and JLab [7], however, the total cross sections of the CLAS data were obtained from a Legendre fit to the angular distributions.

In Fig. 3 the new fit is shown for total cross sections of  $\eta$  and  $\eta'$  photoproduction on the proton target. In both cases also the flat Regge contribution is plotted, which is rather small for energies below  $W \approx 2$  GeV. However, it also interferes with same partial waves for the total cross sections. For angular distributions, the interferences among different resonance contributions and the Regge background become very important. In our fit to the Mainz, Bonn, GRAAL and JLab data we have found significant sensitivity to 18  $N^*$  resonances:  $P_{11}(1440)$ ,  $D_{13}(1520)$ ,  $S_{11}(1535)$ ,  $S_{11}(1650)$ ,  $D_{15}(1675)$ ,  $F_{15}(1680)$ ,  $D_{13}(1700)$ ,  $P_{11}(1710)$ ,  $P_{13}(1720)$ ,  $F_{15}(1860)$ ,  $D_{13}(1875)$ ,  $P_{11}(1880)$ ,  $S_{11}(1895)$ ,  $P_{13}(1900)$ ,  $F_{15}(2000)$ ,  $D_{15}(2060)$ ,  $D_{13}(2120)$ ,  $G_{17}(2190)$ . Overall, we obtained a very good fit to all data on diff. cross sections and polarization observables. The total cross sections themselves are not fitted, they are the result of the partial wave analysis.

## References

- [1] D. Drechsel, O. Hanstein, S. S. Kamalov and L. Tiator, Nucl. Phys. A **645**, 145 (1999) <http://www.kph.uni-mainz.de/MAID/>
- [2] W. T. Chiang, S. N. Yang, L. Tiator and D. Drechsel, Nucl. Phys. A **700**, 429 (2002)
- [3] W. T. Chiang et al., Phys. Rev. C **68**, 045202 (2003)
- [4] M. Ostrick, Proc. 10th Int. Workshop on the Physics of Excited Nucleons (NSTAR2015) JPS Conf. Proc. 10, 010004 (2016)
- [5] J. Akondi *et al.* (A2 Collaboration at MAMI), Phys. Rev. Lett. **113**, 102001 (2014)
- [6] V. Crede *et al.* (CBELSA/TAPS Collaboration), Phys. Rev. C **80**, 055202 (2009)
- [7] M. Williams *et al.* (CLAS Collaboration), Phys. Rev. C **80**, 045213 (2009)
- [8] O. Bartalini *et al.* (The GRAAL Collaboration), Eur. Phys. J. A **33**, 169 (2007)
- [9] A. Donnachie and Y. S. Kalashnikova, Phys. Rev. C **93**, 025203 (2016)
- [10] W. Braunschweig et al., Phys. Lett. B **33**, 236 (1970)
- [11] J. Dewire et al., Phys. Lett. B **37**, 326 (1971)
- [12] K. A. Olive *et al.* (Particle Data Group), Chin. Phys. C **38**, 090001 (2014)
- [13] A. V. Anisovich et al., Eur. Phys. J. A **48**, 15 (2012)